catalysts

MDPI

Article

Atomic Layer Deposition Coated Filters in Catalytic Filtration of Gasification Gas

Tyko Viertiö [1,*], Viivi Kivelä [1], Matti Putkonen [2], Johanna Kihlman [1] and Pekka Simell [1]

[1] VTT Technical Research Centre of Finland Ltd., P.O. Box 1000, FIN-02044 Espoo, Finland; viivipkivela@gmail.com (V.K.); johanna.kihlman@vtt.fi (J.K.); pekka.simell@vtt.fi (P.S.)
[2] Department of Chemistry, University of Helsinki, P.O. Box 55, FIN-00014 Helsinki, Finland; matti.putkonen@helsinki.fi
* Correspondence: tyko.viertio@vtt.fi

Abstract: Steel filter discs were catalytically activated by ALD, using a coating of supporting Al_2O_3 layer and an active NiO layer for gas cleaning. Prepared discs were tested for model biomass gasification and gas catalytic filtration to reduce or eliminate the need for a separate reforming unit for gasification gas tars and lighter hydrocarbons. Two different coating methods were tested. The method utilizing the stop-flow setting was shown to be the most suitable for the preparation of active and durable catalytic filters, which significantly decreases the amount of tar compounds in gasification gas. A pressure of 5 bar and temperatures of over 850 °C are required for efficient tar reforming. In optimal conditions, applying catalytic coating to the filter resulted in a seven-fold naphthalene conversion increase from 7% to 49%.

Keywords: atomic layer deposition (ALD); gasification gas; tar reforming; catalytic filtration

Citation: Viertiö, T.; Kivelä, V.; Putkonen, M.; Kihlman, J.; Simell, P. Atomic Layer Deposition Coated Filters in Catalytic Filtration of Gasification Gas. *Catalysts* **2021**, *11*, 688. https://doi.org/10.3390/catal11060688

Academic Editor: Morris D. Argyle

Received: 29 April 2021
Accepted: 25 May 2021
Published: 29 May 2021

1. Introduction

Global warming and the availability of fossil fuels are drivers of the development of novel biomass-to-liquid concepts. Biomass gasification has gained attention as a flexible technology for the conversion of biomass to syngas, a mixture of carbon monoxide CO and hydrogen H_2. Liquid transportation fuels can be produced from syngas via, for example, Fischer-Tropsch (FT), methanol or dimethyl ether synthesis [1].

However, these catalytic processes require the feed syngas to be pure of different contaminants [1,2]. Due to the heterogeneous nature of the gasification feedstock and the variations between gasification process designs, the amount of impurities in the generated gasification gases varies greatly [3,4]. Requirements set by the end use of the syngas or downstream process steps determine the amount of impurities tolerated in the cleaned gas [2,5]. For syngas to be used as an FT synthesis feed, practically, the complete removal of impurities, including tar compounds, is required to avoid the deactivation of the FT catalyst [5,6].

The main compounds of syngas derived from biomass gasification gas include H_2, CO, carbon dioxide CO_2, methane CH_4 and steam H_2O [1]. The most important impurities include sulfur compounds, condensable hydrocarbons referred to as tars, ammonia, solid particulates, alkali compounds and chlorine [2,7]. Different gas cleaning technologies include, for example, sulfur adsorption, tar reforming, oxidation or cracking, selective oxidation of ammonia and filtration for solid particles removal [2]. These and other technologies and economics of biomass gasification gas cleaning have been extensively presented and reviewed elsewhere [1,2,8–10].

The reforming of tar compounds, as well as methane, is also preferred in order to increase the yield of syngas and decrease the coking tendencies of downstream processes [10]. Typically, nickel, iron and noble-metal-based catalysts, as well as naturally occurring catalysts such as dolomite, are the materials most studied for the catalytic steam reforming

of tar compounds in gasification gas [4,7,10–12]. Novel combinations are also explored in model compound studies [13].

Hot gas filtration is utilized for the removal of particulate matter and alkali chlorides from syngas, typically at the temperature range of 400–600 °C [2,8]. Cost savings of 5% can be achieved by performing the filtration at a higher temperature of over 800 °C, since the previous and following unit operations—gasification and reforming, respectively—are performed at the higher temperature as well [8]. By adding catalytic functionality to the filter, the reforming of tar and methane can also be performed during filtration to increase the process performance or completely eliminate the need for a separate reforming unit [10,14–28]. A lifetime of at least 1–2 years is required for reforming the catalyst used in hydrogen or methane production from biomass in order to be economically feasible [8]. Catalytic filters could act as a pre-reformer to increase performance and minimize coke formation in the actual reforming unit [10].

Different setups for catalytic filters have been studied, including a fixed catalyst bed [14] or a catalytic foam [18] inside the filter candle. However, the catalytic coating of filter elements instead of a separate catalytic material bed has the advantage of being a simpler filter structure, thus enabling a reduction in manufacturing costs [18].

The challenge in the preparation of the catalytically coated filters is the low surface area, in the order of 0.3 m^2/g, of the filter media. This acts as a catalyst support, and thus limits the surface area of the active metal and therefore causes low activity, especially in the presence of sulfur compounds [21,25]. The deposition of a highly dispersed support layer has been proposed to increase the surface area of the filter media, thus allowing a higher loading of active metal [21,25]. Zhao et al. [26] compared different deposition methods for the nickel in α-Al_2O_3 filter substrates, and found that deposition–precipitation with urea provides more uniform coatings. As with traditional impregnation methods, most of the catalyst metal was found in the outer pores of the filter material.

Atomic layer deposition (ALD) is a mainstream deposition technology in microelectronics, but it has also attracted attention in catalyst preparation, as summarized by Haukka et al. and O'Neill et al. [29,30]. Recently, it has been reported that ALD can be used for the preparation of exceptionally dispersed and stable high metal loading and low-particle size Ni catalysts [31,32]. These observations suggest that ALD as a preparation method could provide a solution for the observed problems in the distribution of the precursor in the preparation of Ni-coated catalytic filters for gasification gas filtration.

In this work, ALD was utilized in the preparation of catalytic filters for gasification gas cleaning by coating steel filter elements to produce catalytic filters with activity in tar reforming. The performance was compared to filters without a catalytic coating. To the best of our knowledge, this was the first time that ALD had been used and tested for the preparation of catalytic filters for the described application.

2. Results and Discussion

2.1. Filters without a coating

The activity results for blank steel filters are presented in Figures 1–3. Compared to the empty quartz reactor equipped with the sinter, the addition of a filter to the reactor did not significantly affect the measured conversions.

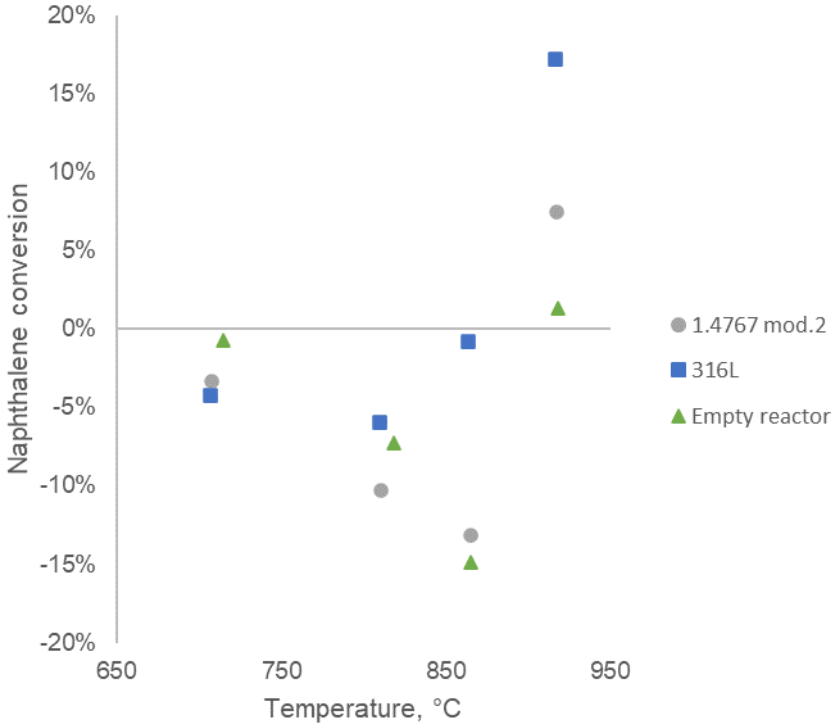

Figure 1. Naphthalene conversion on blank filters, 5 bar, total feed flowrate of 1 L_n/min.

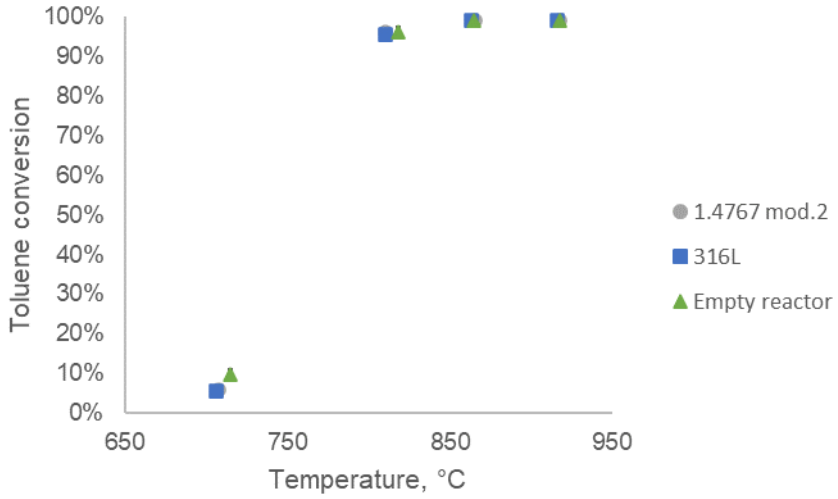

Figure 2. Toluene conversion on uncoated filters, 5 bar, total feed flowrate of 1 L_n/min.

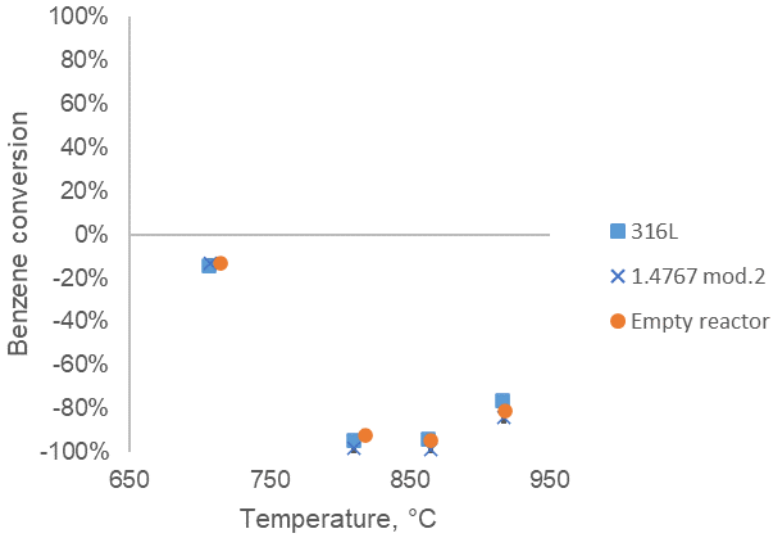

Figure 3. Benzene conversion on uncoated filters, 5 bar, total feed flowrate of 1 L_n/min.

Negative conversions were observed especially at a pressure of 5 bar and lower temperatures due to the thermal formation of the measured tar compounds. Instead of decomposition, tar compounds can be formed in thermal reactions in the presence of lower-molecular-weight tars [33] and ethene [34]. Thus, the amount of the measured component is higher in the reactor outlet than in the inlet. Consequently, the formation of a component causes negative conversion, according to Equation 1. Ethene conversions of 30–100% were indeed detected, as shown in Figure 4. The sinter of the quartz reactor has to be taken into account in the evaluation of the tests. The sinter provides filter-like reaction conditions for the thermal reactions in every experiment.

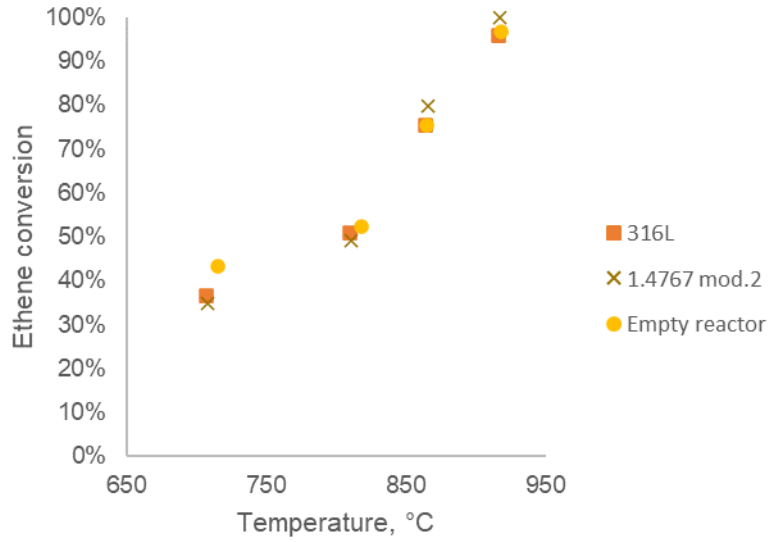

Figure 4. Ethene conversion on uncoated filters, 5 bar, total feed flowrate of 1 L_n/min.

In addition to thermal tar formation, the negative conversion of benzene is caused by the thermal decomposition of toluene to benzene and methane [35], as almost full conversion is found at elevated pressure at 800 °C regardless of the filter, as seen in Figure 2. Based on these results, the evaluation of the performance of different catalysts is based on naphthalene conversion.

A minor increase was detected in the conversion of naphthalene on the 316L steel filter at higher temperatures of 860 °C and 920 °C. The increase was attributed to the catalytic activation of the nickel-containing steel material at temperatures higher than 850 °C, as

reported earlier by Abbas and Daud [36] in the thermocatalytic decomposition of methane. The catalytic activation of the steel surface is also supported by the fact that the addition of alumina coating to the steel filter decreased the detected catalytic activity.

2.2. Filters Coated with the Flow-Through Method

When compared to blank filters, no significant increase in the conversion of tar compounds was achieved with the NiO-coated filters coated using the forced-flow method, as seen in Figure 5.

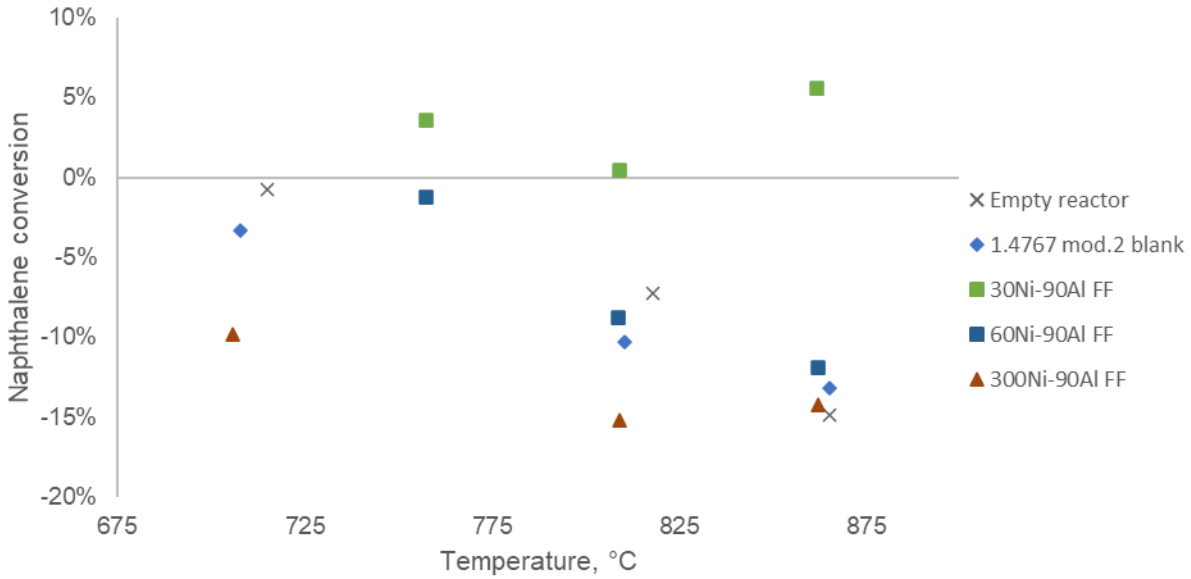

Figure 5. Naphthalene conversion on flow-through coated filters, 5 bar, total feed flowrate of 1 L_n/min.

The elemental analysis of the forced-flow coated filters using SEM-EDS showed the amount of nickel on the top side of the filter to be a function of the number of deposition cycles, as expected. The amount of nickel varied from 1 wt. % to 14 wt. % for filters with 30 cycles and 300 cycles of NiO, respectively. However, on the bottom side of the filter, no nickel was detected. Most probably, the plate tool used had not been effective enough to force the flow through the filter during the deposition. The flow bypassing the filter explains why no nickel was detected on the bottom side and only the top side, which is easily accessible to the precursors, was coated. In addition, the low amount of nickel can be partly attributed to the low dose of the metal precursor and the decomposition of ozone on the metallic materials while gases were passed through the filter. Decomposition of O_3 on metallic surfaces has been previously observed, which would also limit the amount of nickel deposited in the filter [37,38]. The low overall amount of nickel combined with the low surface area of the filters could explain the low activity of the filters in catalytic filtration.

2.3. Filters Coated with the Stop-Flow Method

The stop-flow setting was utilized to increase the amount of nickel in the coating. In addition, the number of NiO ALD cycles was increased. A significant increase in the catalytic activity was achieved by the catalytic nickel coating of 800 or 1600 cycles of NiO. The results obtained by the activity tests of these filters at 5 bar and 1 L_N/min are presented in Figure 6.

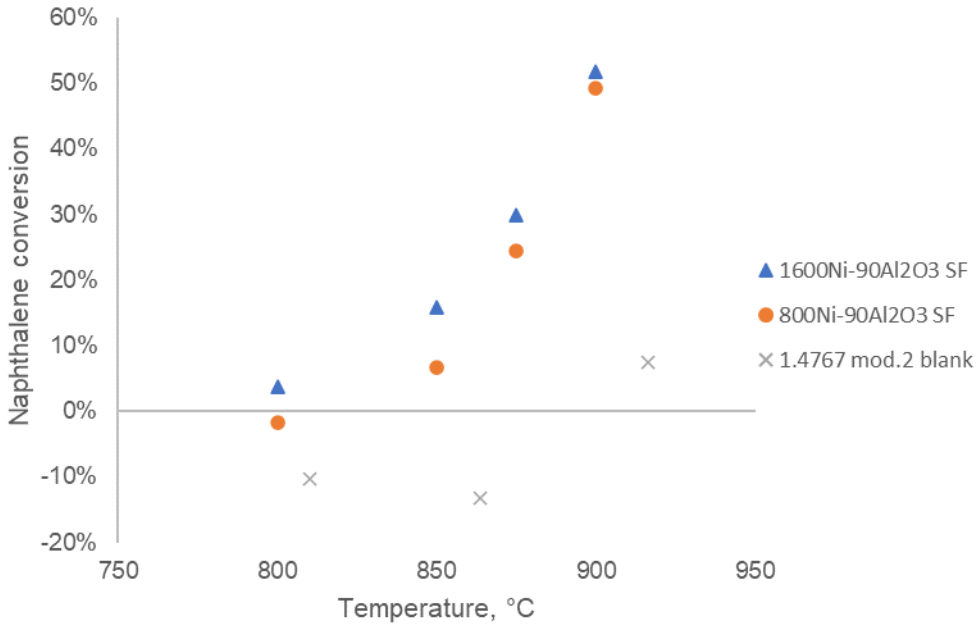

Figure 6. Naphthalene conversion on Ni-coated filters by stop-flow method, 5 bar, total feed flowrate of 1 L_n/min.

The Ni ALD coating significantly increased the conversion of naphthalene in the catalytic filtration, as shown in Figure 6. The increase in the amount of nickel on the filter from 800 to 1600 cycles did not significantly increase the naphthalene decomposition activity under the experimental conditions. This is probably due to the low surface area of the filters, as the increase in nickel in the filter did not increase the active nickel surface area. Similar results of the effect of varying the amount of deposited catalyst material on a low-surface area filter have been reported by Zhang et al. [25].

Figure 7 presents the conversions of the filter with 800 cycles of Ni compared to an uncoated filter at 900 °C and 5 bar. As can be seen, in addition to a drastic increase in naphthalene conversion, the decomposition of benzene is also significantly increased with the introduction of the catalyst.

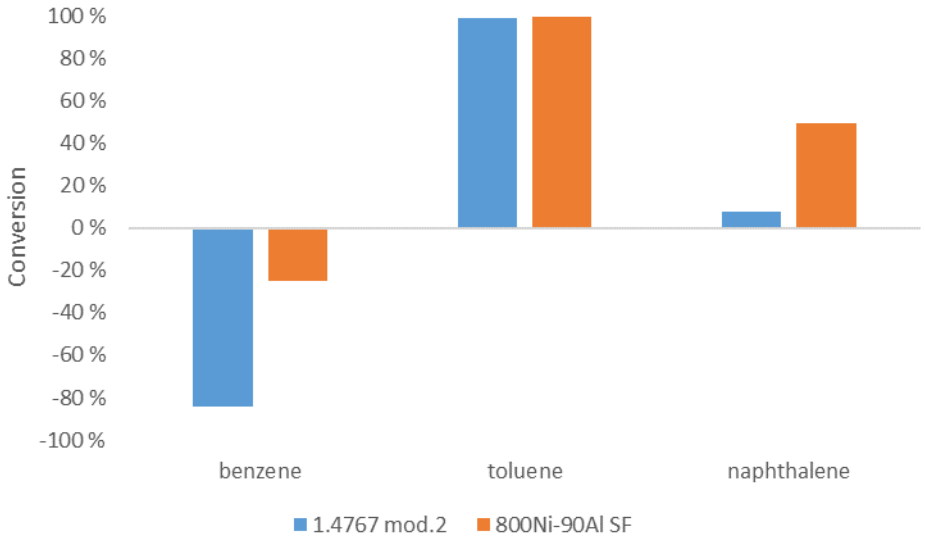

Figure 7. Comparison of conversions of uncoated filter with a filter with 800 cycles of nickel and 90 cycles of Al_2O_3 at 900 °C and 5 bar.

Additionally, the effect of lowering the number of ALD cycles was tested without the Al_2O_3 support coating. Naphthalene decomposition activity was detected, but it

was significantly lower than with the support, either due to the lack of support or the lower amount of catalytically active nickel. The results of the lower amount of nickel are presented in Figure 8.

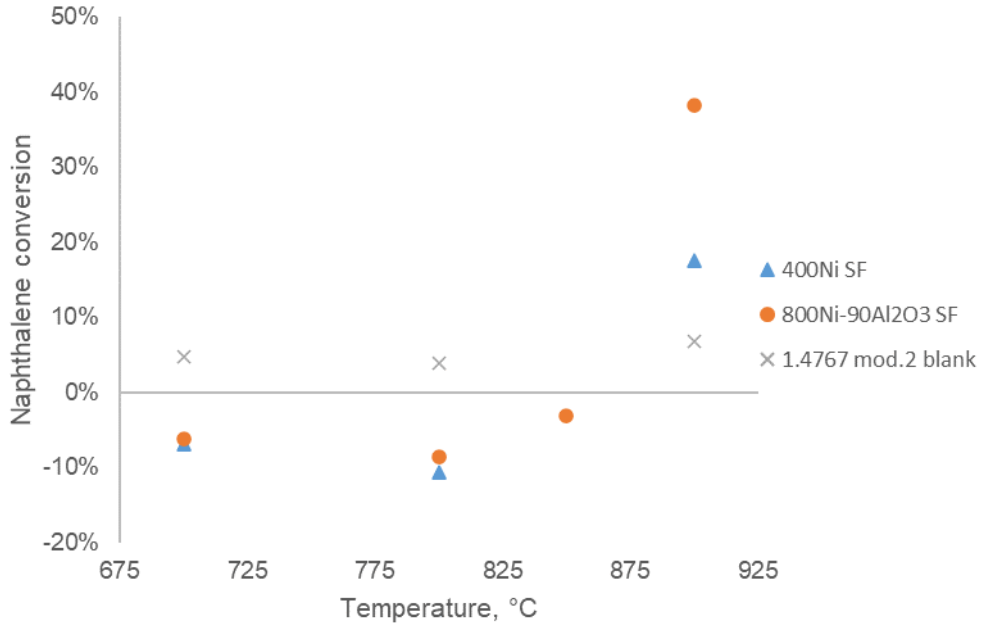

Figure 8. Naphthalene conversion on stop-flow coated filters, 5 bar, total feed flowrate of 1.5 L_n/min.

2.4. Effect of Process Conditions

The catalysts were also tested at pressures of 1 and 3 bar. However, the conversions of the catalytic and thermal reactions were low in these conditions when compared to 5 bar, especially at around 800 °C, as seen in Figures 9 and 10. A similar trend was observed both with a low amount of the catalyst and with no catalyst. Naphthalene conversion can be seen to be insignificant, except at 900 °C and 5 bar. According to these results, the elevated pressure of 5 bar is recommended.

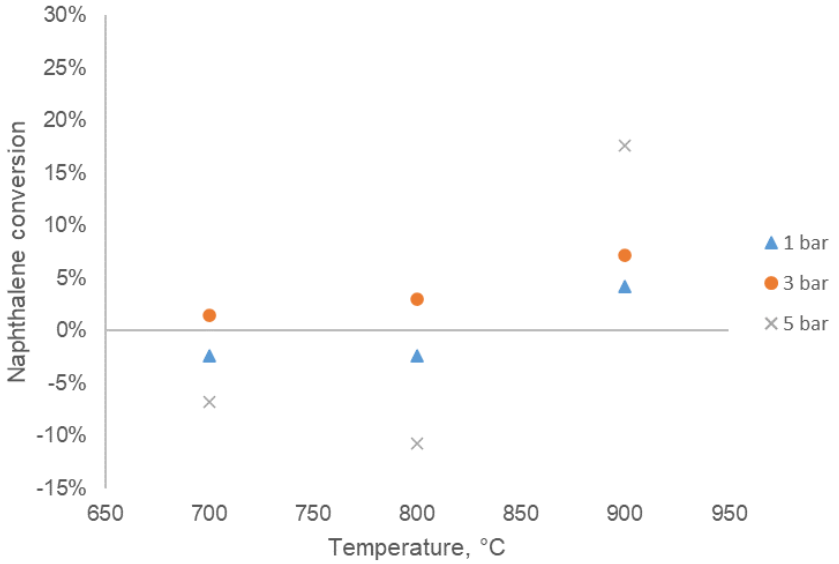

Figure 9. Naphthalene conversion on stop-flow coated filter with 400 cycles of Ni at different pressures, total feed flowrate of 1.5 L_n/min.

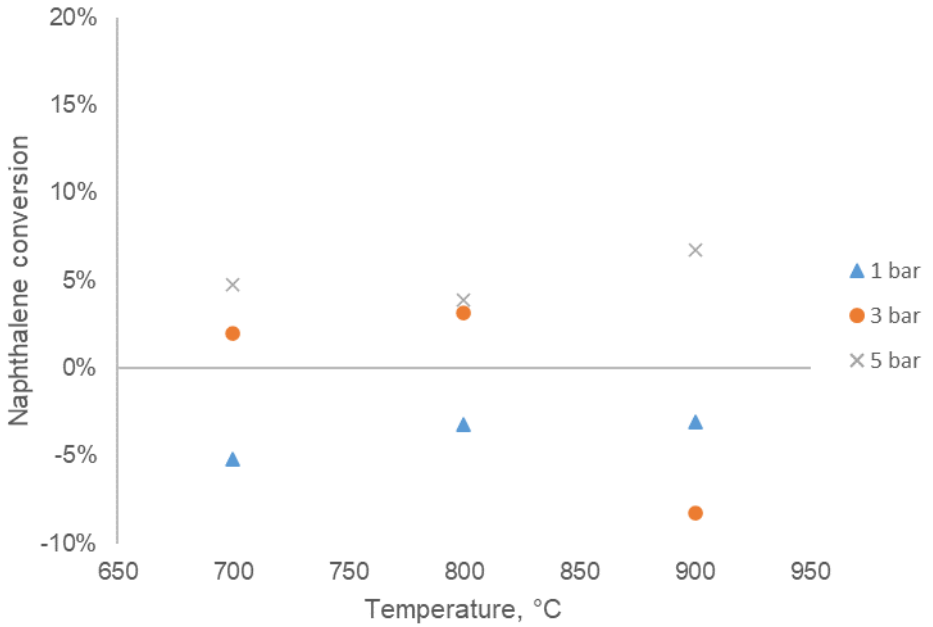

Figure 10. Naphthalene conversion on filter without catalyst at different pressures, total feed flowrate of 1.5 L_n/min.

The effect of flowrate was studied at a pressure of 5 bar. As stated earlier, the limitations of the experimental setup limited the feed gas flowrate to 0.75–1.5 L_n/min, corresponding to face velocities of 9–20 cm/s. When the gas flowrate was varied, no significant difference was observed in naphthalene conversion, as seen in Figure 11. Most probably, the formation of naphthalene from lower-molecular-weight tars increased simultaneously with the reforming activity when the feed flowrate was decreased, increasing the residence time in the filter.

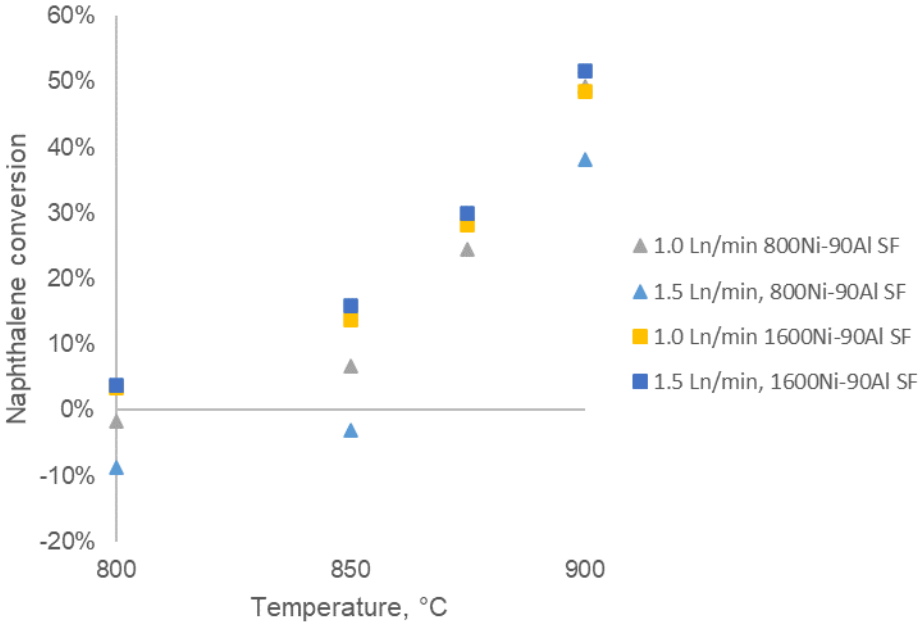

Figure 11. Naphthalene conversion on stop-flow coated filters with different feed flowrates, 5 bar.

2.5. Deactivation Due to Sulfur Poisoning and Coke Formation

Sulfur compounds formed in biomass gasification were modeled using 60 ppm of H_2S in the feed gas, which simulates the content in a biomass gasification gas [8]. To monitor the effect of sulfur on the prepared catalytic filters, one test run was performed without a

sulfur feed, as presented in Figure 12. The effect of the sulfur was pronounced at lower temperatures, especially at 700 °C. At higher temperatures, the conversion of naphthalene remains similar to the non-sulfur-containing feed. The reason for this behavior is that the adsorption of sulfur to active sites decreases at high temperatures [39], causing an increase in naphthalene conversion.

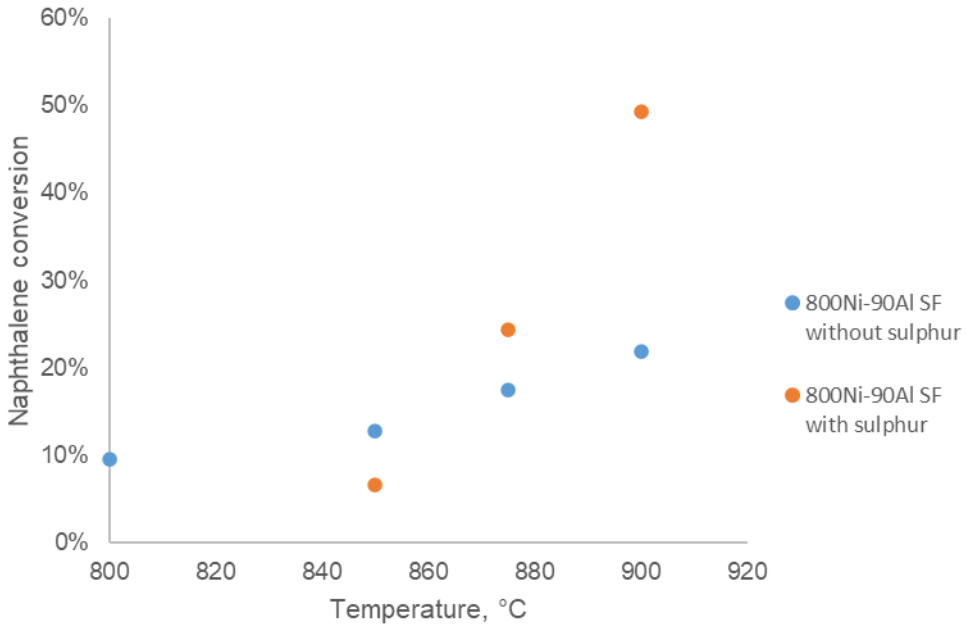

Figure 12. Naphthalene conversion with and without H_2S in the feed on stop-flow coated filter, 5 bar, total feed flowrate of 1 L_n/min.

Coke formation on the filter and reactor walls took place in all the test runs. However, the highest amounts of carbon were formed in the experiments where significant naphthalene conversion was observed, which is probably due to the partial decomposition of naphthalene to coke [40]. Coke formation was observed to cause an increase in the pressure drop and eventually led to reactor clogging at higher temperature settings of over 850 °C. However, no decrease in catalyst activity was detected due to the coke formation on the filter. Further studies are required to minimize the effect of coke formation, especially when combined with the particulate matter of real biomass gasification gas and filter regeneration.

3. Materials and Methods

3.1. Filters

Steel filter discs prepared from 1.4767 mod.2 and 316L stainless steel grades, were provided by GKN Sinter Metals Filters GmbH (Radevormwald, Germany). The most important difference between the alloys is the amount of nickel: 0 and 10–14 w. % of Ni for steel alloys 1.4767 mod.2 and 316L, respectively. Filters were 3 mm thick discs with diameters of 25 mm. The specific surface area for filter materials was 0.40–0.54 m^2/g, depending on the filter type. The typical weight of the filters was 5.5–6.2 g. The properties of the different filters are presented in Table 1.

Table 1. Catalytic filter material compositions provided by the manufacturer.

Steel Material	Cr, w. %	Ni, w. %	In Addition
1.4767 mod.2	19–22	-	<0.1 w. % of C, 5–6 w. % of Al with rare earths
AISI 316L	16–18	10–14	<0.03 w. % of C, 2–3 w. % of Mo

3.2. ALD Coatings

ALD coatings for filters were conducted in a Picosun SUNALE R-200 ALD reactor (Picosun Oy, Espoo, Finland). N_2 (99.9999%, AGA, Espoo, Finland) was used as the inert purge and carrier gas. For the deposition of Al_2O_3 layers, trimethylaluminum (TMA) (SAFC, purity 99%, St. Louis, MO, USA) and H_2O were used as precursors. Nickel oxide coatings were deposited using bis(2,2,6,6-tetramethylheptane-3,5- dionato)nickel(II) ($Ni(thd)_2$) and O_3 as precursors. $Ni(thd)_2$ (Strem Chemicals, 98%, Newburyport, MA, USA) was sublimated at 175 °C. O_3 was generated from oxygen (99.999%) provided by AGA in an IN USA, Inc. (Norwood, MA, USA) ozone generator.

All depositions were performed at 225 °C. Additional silicon wafer pieces were used to measure the thickness of the deposited layer and to monitor the uniformity of the deposition in different parts of the reactor chamber. The thicknesses of the films deposited on the monitor Si pieces were measured using ellipsometry (Sentech SE400adv tool, SENTECH Instruments GmbH, Berlin, Germany).

For the Al_2O_3 coatings, the filter discs were positioned on a metal stand with a height of 6 mm providing free gas flow from both sides of the discs and the diffusion of the precursor to the pores of the filters. Pulse times of 0.5, 0.5, 9.0 and 3.0 s were used for TMA, H_2O, $Ni(thd)_2$ and O_3, respectively.

The stop-flow setting of the Picosun tool was used to increase the diffusion of the precursors inside the filter. During the stop-flow setting, the removal of the precursors from the reactor is stopped during the precursor pulse for a given time, 5 s in these experiments, to increase the residence time of the precursor and therefore promote precursor diffusion to the inner parts of the filter pores. Subsequently, Al_2O_3 deposition filters were exposed to air before the NiO depositions, but no additional treatments were carried out.

Two deposition methods were tested for NiO coatings, and are schematically described in Figure 13. In the forced-flow method, a plate tool was installed in the reactor, with the aim of forcing the precursor flow through the filter to promote the deposition of the precursor to the walls of the filter pores inside the filter. The number of ALD cycles for the forced-flow coated filters was 30–300, and each reaction step consisted of five consecutive pulses of nickel precursor or ozone.

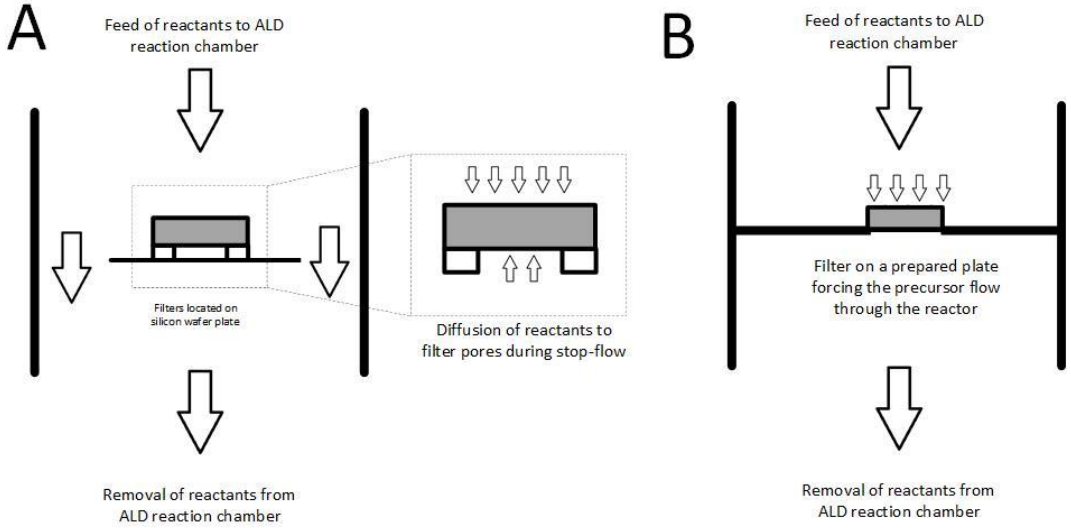

Figure 13. Schematic description of the preparation methods: (**A**) stop-flow method; (**B**) forced-flow method.

In the stop-flow method, a stop-flow setting of 5 s and a metal stand were used, as used in the Al_2O_3 coatings. The number of ALD cycles tested varied between 400 and 1600. The list of prepared filters with ALD parameters and ellipsometry results is presented in Table 2.

Table 2. List of prepared filters.

Filter Name	Steel Material	Number of TMA-H_2O Cycles	Number of $Ni(thd)_2$-O_3 Cycles	Pulses Per Cycle of $Ni(thd)_2$ or O_3	Stop-Flow in Use in NiO Deposition	Forced-Flow	Measured NiO Layer Thickness on Si Pieces (nm)
1.4767 mod.2 blank	1.4767 mod.2	-	-	-	-	-	-
316L blank	316L	-	-	-	-	-	-
30Ni-90Al FF	1.4767 mod.2	90	30	5	No	Yes	3.6–4.3
60Ni-90Al FF	1.4767 mod.2	90	60	5	No	Yes	5.9–18.1
300Ni-90Al FF	1.4767 mod.2	90	300	5	No	Yes	10.6–13.2
400Ni SF	1.4767 mod.2	-	400	1	Yes, 5 sec	No	16–18
800Ni-90Al SF	1.4767 mod.2	90	800	1	Yes, 5 sec	No	35–39
1600Ni-90Al SF	1.4767 mod.2	90	1600	1	Yes, 5 sec	No	60–65

3.3. Activity Tests

The prepared filters were tested for catalytic activity in a laboratory-scale reactor. The general design of the experimental setup is presented in Figure 14. Temperatures ranging from 700 to 920 °C, absolute pressures ranging from 1 to 5 bar and gas flowrates of 0.75–1.5 L_N/min were studied. Due to the limitations of the equipment, the tested flowrate led to filtration face velocities of 9–21 cm/s and gas hourly space velocities (GHSV) of 30 000–60 000 h^{-1}, which was significantly higher than the industrially relevant gas face velocity (defined as volumetric flowrate per filter outside surface area) of 1–5 cm/s, often reported by other researchers [18,21].

The quartz reactor consisted of two parts, with a sinter in the middle of the top section of the lower reactor part. The filter was packed on top of the sinter and quartz wool was used to tighten the filter to the reactor and direct the gas flow through the filter. The diameter of the reactor at the location of the filter was 27 mm and the full length of the reactor was 35 or 40 cm. The quartz reactor setup and filter are presented in Figure S1. The reaction temperature was measured by a thermocouple located on the exit surface of the reaction gas from the filter. The temperature setting was changed from lower temperatures to higher in periods of 4 h. Before each run, the catalyst was reduced under a 1:1 H_2:N_2 flow of 1.0 L/min at 1 bar and at 750 or 800 °C for 1 h.

The feed gas composition was based on practical industrial and pilot knowledge of the composition of steam gasification gas and is presented in Table 3 [8]. Toluene, benzene and naphthalene were used as tar model compounds, and were provided by Merck (Darmstadt, Germany). The gases were provided by AGA (Espoo, Finland). The gases were fed from separate gas bottles and were controlled by Bronckhorst mass flow controllers (BRONKHORST HIGH-TECH B.V., Ruurlo, Netherlands). The tar model compound solution and ion-exchanged water were fed into the system as liquids through the vaporizer and controlled by high-performance liquid chromatography (HPLC) pumps.

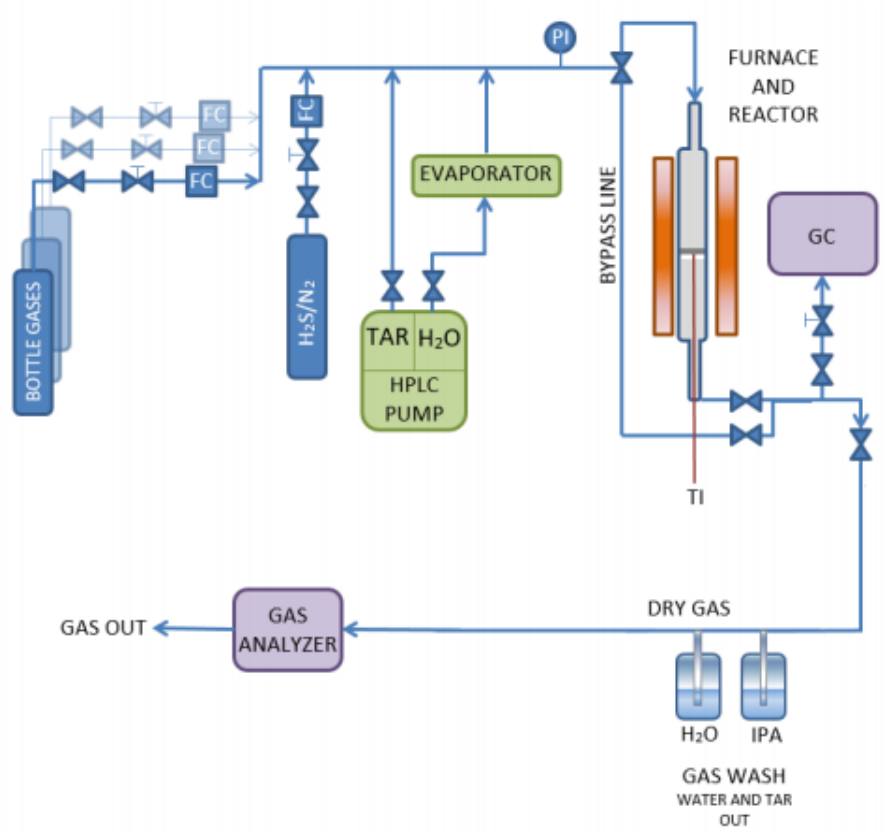

Figure 14. General design of the experimental setup (Figure by VTT Technical Research Center of Finland).

Table 3. Feed gas composition.

Compound.	Vol. %	Purity (%)
CO	10.7	99.97
CO_2	15.5	99.99
CH_4	2.8	99.995
H_2	22.7	99.999
C_2H_4	1.7	99.95
H_2O	44.3	-
N_2	2.0	Generated from industrial liquid nitrogen
Compound	vol-ppm	Purity
benzene	1715	99.7
toluene	1670	99.9
naphthalene	223	99
H_2S	60	0.5000 mol. % in N_2

The composition of the outlet gas was analyzed using online gas chromatography and an online gas analyzer. Depending on the reactor setup, an Agilent 7890 GC (Agilent, Santa Clara, CA USA) equipped with two FID detectors with an HP-5 column and either an HP-PLOT-Q or a GS-GASPRO column was utilized for the detection of the tar compounds and hydrocarbons. In addition, depending on the reactor setup, either a SICK-Maihak-type S710 or an ABB AO2020 online gas analyzer was used for the detection of CO, CO_2, CH_4, H_2 and O_2.

The results were calculated by fitting the elemental balances of carbon, hydrogen and oxygen. The conversions of the components were calculated according to Equation (1). Carbon elemental balance closures of 91% to 106% were received for all temperature settings.

$$X_i = \frac{F_{i,IN} - F_{i,OUT}}{F_{i,IN}} \quad (1)$$

where $F_{i,IN/OUT}$ is the molar flow of component i to the reactor and from the reactor (mol/s).

3.4. Characterization

Scanning electron microscopy (SEM) combined with energy-dispersive X-ray spectrometry (EDS) was used in the elemental analysis of the prepared catalytic filters. Analysis was conducted using a Merlin scanning electron microscope (ZEISS, Oberkochen, Germany) equipped with a ThermoFisher (Waltham, MA, USA) UltraDry spectrometer (Silicon drift detector). SEM-EDS results were analyzed using ThermoFisher NSS 3.2.298 software (Madison, WI, USA, 2013).

4. Conclusions

The potential of ALD as a preparation method for catalytic filters was demonstrated for catalytic filtration with Al_2O_3- and NiO-coated steel filters. Reasonably good catalytic activity with extremely high face velocity in naphthalene decomposition was detected with the stop-flow coated filters used in the decomposition of gasification gas tar. Optimal performance was achieved with filters containing 35–39 nm (800 cycles) of nickel oxide on top of an alumina layer. Temperatures close to 900 °C and a pressure of 5 bar are required for efficient naphthalene conversion. The naphthalene conversion increased from 7% to 49% following the application of the catalytic coating compared to a blank filter at 900 °C and 5 bar, and a significant decrease in benzene in the tests with catalytic filters was also detected.

Further studies are required to optimize the loading of the catalyst to the filter, as well as the minimization of coke formation and the filter behavior with a real gasification gas feed. However, catalytic filter coating by ALD shows promising results for future research into gasification gas cleaning or other chemical industry applications.

Supplementary Materials: The following are available online at https://www.mdpi.com/article/10.3390/catal11060688/s1, Figure S1: Reactor configuration and the filter packing.

Author Contributions: Conceptualization, J.K., P.S. and M.P.; methodology, V.K. and T.V; validation, V.K., T.V, M.P., J.K. and P.S.; formal analysis, T.V. and V.K.; investigation, V.K., T.V. and M.P.; resources, V.K., T.V. and M.P.; data curation, T.V. and V.K.; writing—original draft preparation, V.K. and T.V.; writing—review and editing, J.K., P.S. and M.P.; visualization, V.K. and T.V.; supervision, J.K. and P.S.; project administration, J.K. and P.S.; funding acquisition, J.K. and P.S. All authors have read and agreed to the published version of the manuscript.

Funding: COMSYN project has received funding from the European Union's Horizon 2020 research and innovation program under grant agreement No 727476. M.P. acknowledges funding from the Academy of Finland through the profiling action on Matter and Materials, grant no. 318913.

Acknowledgments: COMSYN project has received funding from the European Union's Horizon 2020 research and innovation program under grant agreement No 727476. M.P. acknowledges funding from the Academy of Finland through the profiling action on Matter and Materials, grant no. 318913. Sanna Tuomi (VTT) and Harald Balzer (GKN Sinter Metals) are acknowledged for their expert views on the topic, and Patrik Eskelinen, Katja Heiskanen, Petri Hietula, Päivi Jokimies, Mari-Leena Koskinen-Soivi, Mirja Muhola and Johannes Roine for their support during the analyses and practical issues experienced during the research work. Riikka Puurunen and Ville Alopaeus (Aalto University) are acknowledged for their supervision of related master's thesis projects.

Conflicts of Interest: The authors declare no conflict of interest.

References

1. Sikarwar, V.S.; Zhao, M.; Clough, P.; Yao, J.; Zhong, X.; Memon, M.Z.; Shah, N.; Anthony, E.J.; Fennell, P.S. An overview of advances in biomass gasification. *Energy Environ. Sci.* **2016**, *9*, 2939–2977. [CrossRef]
2. Woolcock, P.J.; Brown, R.C. A review of cleaning technologies for biomass-derived syngas. *Biomass Bioenergy* **2013**, *52*, 54–84. [CrossRef]
3. Kurkela, E.; Kurkela, M.; Hiltunen, I. Steam-oxygen gasification of forest residues and bark followed by hot gas filtration and catalytic reforming of tars: Results of an extended time test. *Fuel Process. Technol.* **2016**, *141*, 148–158. [CrossRef]
4. Rios, M.L.V.; González, A.M.; Lora, E.E.S.; del Olmo, O.A.A. Reduction of tar generated during biomass gasification: A review. *Biomass Bioenergy* **2018**, *108*, 345–370. [CrossRef]
5. Hu, J.; Yu, F.; Lu, Y. Application of Fischer–Tropsch Synthesis in Biomass to Liquid Conversion. *Catalysts* **2012**, *2*, 303–326. [CrossRef]
6. Tijmensen, M.J. Exploration of the possibilities for production of Fischer Tropsch liquids and power via biomass gasification. *Biomass Bioenergy* **2002**, *23*, 129–152. [CrossRef]
7. Abdoulmoumine, N.; Adhikari, S.; Kulkarni, A.; Chattanathan, S. A review on biomass gasification syngas cleanup. *Appl. Energy* **2015**, *155*, 294–307. [CrossRef]
8. Simell, P.; Hannula, I.; Tuomi, S.; Nieminen, M.; Kurkela, E.; Hiltunen, I.; Kaisalo, N.; Kihlman, J. Clean syngas from biomass—process development and concept assessment. *Biomass Convers. Biorefinery* **2014**, *4*, 357–370. [CrossRef]
9. Yung, M.M.; Jablonski, W.S.; Magrini-Bair, K.A. Review of Catalytic Conditioning of Biomass-Derived Syngas. *Energy Fuels* **2009**, *23*, 1874–1887. [CrossRef]
10. Kaisalo, N.; Kihlman, J.; Hannula, I.; Simell, P. Reforming solutions for biomass-derived gasification gas—Experimental results and concept assessment. *Fuel* **2015**, *147*, 208–220. [CrossRef]
11. Anis, S.; Zainal, Z. Tar reduction in biomass producer gas via mechanical, catalytic and thermal methods: A review. *Renew. Sustain. Energy Rev.* **2011**, *15*, 2355–2377. [CrossRef]
12. Rönkkönen, H.; Simell, P.; Reinikainen, M.; Krause, O.; Niemelä, M.V. Catalytic clean-up of gasification gas with precious metal catalysts—A novel catalytic reformer development. *Fuel* **2010**, *89*, 3272–3277. [CrossRef]
13. Jayaprakash, S.; Dewangan, N.; Jangam, A.; Kawi, S. H2S-resistant CeO2-NiO-MgO-Al2O3 LDH-derived catalysts for steam reforming of toluene. *Fuel Process. Technol.* **2021**, *219*, 106871. [CrossRef]
14. Nacken, M.; Ma, L.; Engelen, K.; Heidenreich, S.; Baron, G.V. Development of a Tar Reforming Catalyst for Integration in a Ceramic Filter Element and Use in Hot Gas Cleaning. *Ind. Eng. Chem. Res.* **2007**, *46*, 1945–1951. [CrossRef]
15. Rapagnà, S.; Gallucci, K.; Di Marcello, M.; Foscolo, P.U.; Nacken, M.; Heidenreich, S. In Situ Catalytic Ceramic Candle Filtration for Tar Reforming and Particulate Abatement in a Fluidized-Bed Biomass Gasifier. *Energy Fuels* **2009**, *23*, 3804–3809. [CrossRef]
16. Rapagnà, S.; Gallucci, K.; Di Marcello, M.; Matt, M.; Nacken, M.; Heidenreich, S.; Foscolo, P.U. Gas cleaning, gas conditioning and tar abatement by means of a catalytic filter candle in a biomass fluidized-bed gasifier. *Bioresour. Technol.* **2010**, *101*, 7123–7130. [CrossRef] [PubMed]
17. Nacken, M.; Ma, L.; Heidenreich, S.; Baron, G.V. Performance of a catalytically activated ceramic hot gas filter for catalytic tar removal from biomass gasification gas. *Appl. Catal. B Environ.* **2009**, *88*, 292–298. [CrossRef]
18. Nacken, M.; Baron, G.V.; Heidenreich, S.; Rapagnà, S.; D'Orazio, A.; Gallucci, K.; Denayer, J.F.; Foscolo, P.U. New DeTar catalytic filter with integrated catalytic ceramic foam: Catalytic activity under model and real bio syngas conditions. *Fuel Process. Technol.* **2015**, *134*, 98–106. [CrossRef]
19. Rapagnà, S.; Gallucci, K.; Di Marcello, M.; Foscolo, P.U.; Nacken, M.; Heidenreich, S.; Matt, M. First Al2O3 based catalytic filter candles operating in the fluidized bed gasifier freeboard. *Fuel* **2012**, *97*, 718–724. [CrossRef]
20. Ma, L.; Baron, G.V. Mixed zirconia–alumina supports for Ni/MgO based catalytic filters for biomass fuel gas cleaning. *Powder Technol.* **2008**, *180*, 21–29. [CrossRef]
21. Nacken, M.; Ma, L.; Heidenreich, S.; Baron, G.V. Catalytic Activity in Naphthalene Reforming of Two Types of Catalytic Filters for Hot Gas Cleaning of Biomass-Derived Syngas. *Ind. Eng. Chem. Res.* **2010**, *49*, 5536–5542. [CrossRef]
22. Engelen, K.; Zhang, Y.; Draelants, D.J.; Baron, G.V. A novel catalytic filter for tar removal from biomass gasification gas: Improvement of the catalytic activity in presence of H2S. *Chem. Eng. Sci.* **2003**, *58*, 665–670. [CrossRef]
23. Ma, L.; Verelst, H.; Baron, G. Integrated high temperature gas cleaning: Tar removal in biomass gasification with a catalytic filter. *Catal. Today* **2005**, *105*, 729–734. [CrossRef]
24. Zhang, Y.; Draelants, D.J.; Engelen, K.; Baron, G.V. Improvement of Sulphur Resistance of a Nickel-modified Catalytic Filter for Tar Removal from Biomass Gasification Gas. In Proceedings of the 5th International Symposium on Gas Cleaning at High Temperatures, Morgantown, WV, USA, 17–20 September 2002.
25. Zhang, Y.; Draelants, D.J.; Engelen, K.; Baron, G.V. Development of nickel-activated catalytic filters for tar removal in H2S-containing biomass gasification gas. *J. Chem. Technol. Biotechnol.* **2003**, *78*, 265–268. [CrossRef]
26. Zhao, H.; Draelants, D.J.; Baron, G.V. Preparation and characterisation of nickel-modified ceramic filters. *Catal. Today* **2000**, *56*, 229–237. [CrossRef]
27. Heidenreich, S.; Nacken, M.; Hackel, M.; Schaub, G. Catalytic filter elements for combined particle separation and nitrogen oxides removal from gas streams. *Powder Technol.* **2008**, *180*, 86–90. [CrossRef]

28. Nacken, M.; Ma, L.; Heidenreich, S.; Verpoort, F.; Baron, G.V. Development of a catalytic ceramic foam for efficient tar reforming of a catalytic filter for hot gas cleaning of biomass-derived syngas. *Appl. Catal. B Environ.* **2012**, *125*, 111–119. [CrossRef]
29. O'Neill, B.J.; Jackson, D.H.K.; Lee, J.; Canlas, C.; Stair, P.C.; Marshall, C.L.; Elam, J.W.; Kuech, T.F.; Dumesic, J.A.; Huber, G.W. Catalyst Design with Atomic Layer Deposition. *ACS Catal.* **2015**, *5*, 1804–1825. [CrossRef]
30. Haukka, S.; Lakomaa, E.-L.; Suntola, T. Adsorption controlled preparation of heterogeneous catalysts. *Stud. Surf. Sci. Catal.* **1999**, *120*, 715–750. [CrossRef]
31. Shang, Z.; Li, S.; Li, L.; Liu, G.; Liang, X. Highly active and stable alumina supported nickel nanoparticle catalysts for dry reforming of methane. *Appl. Catal. B Environ.* **2017**, *201*, 302–309. [CrossRef]
32. Gould, T.D.; Lubers, A.M.; Neltner, B.T.; Carrier, J.V.; Weimer, A.W.; Falconer, J.L.; Medlin, J.W. Synthesis of supported Ni catalysts by atomic layer deposition. *J. Catal.* **2013**, *303*, 9–15. [CrossRef]
33. Tuomi, S.; Kurkela, E.; Simell, P.; Reinikainen, M. Behaviour of tars on the filter in high temperature filtration of biomass-based gasification gas. *Fuel* **2015**, *139*, 220–231. [CrossRef]
34. Kaisalo, N.K.; Koskinen-Soivi, M.-L.; Simell, P.A.; Lehtonen, J. Effect of process conditions on tar formation from thermal reactions of ethylene. *Fuel* **2015**, *153*, 118–127. [CrossRef]
35. Jess, A. Mechanisms and kinetics of thermal reactions of aromatic hydrocarbons from pyrolysis of solid fuels. *Fuel* **1996**, *75*, 1441–1448. [CrossRef]
36. Abbas, H.F.; Daud, W.W. Influence of reactor material and activated carbon on the thermocatalytic decomposition of methane for hydrogen production. *Appl. Catal. A Gen.* **2010**, *388*, 232–239. [CrossRef]
37. Hutchings, G.; Copperthwaite, R.; Themistocleous, T.; Foulds, G.; Bielovitch, A.; Loots, B.; Nowitz, G.; Van Eck, P. A comparative study of reactivation of zeolite Y using oxygen and ozone/oxygen mixtures. *Appl. Catal.* **1987**, *34*, 153–161. [CrossRef]
38. Onn, T.M.; Küngas, R.; Fornasiero, P.; Huang, K.; Gorte, R.J. Atomic Layer Deposition on Porous Materials: Problems with Conventional Approaches to Catalyst and Fuel Cell Electrode Preparation. *Inorganics* **2018**, *6*, 34. [CrossRef]
39. Hepola, J. Sulfur Transformations in Catalytic Hot-Gas Cleaning of Gasification Gas. Ph.D. Thesis, Helsinki University of Technology, Espoo, Finland, December 2000.
40. Gai, C.; Dong, Y.; Yang, S.; Zhang, Z.; Liang, J.; Li, J. Thermal decomposition kinetics of light polycyclic aromatic hydrocarbons as surrogate biomass tar. *RSC Adv.* **2016**, *6*, 83154–83162. [CrossRef]